

Formulation And Evaluation Of Allicin Loaded Nanoparticles For Potential Antiseptic Properties

Fatema Neherwala¹, Dr. (Prof.) M. K. Gupta², Shailesh Kumar³, Alok kumar⁴, Ankit Yadav⁵, Akshay Kumar⁶

Cite this paper as: Fatema Neherwala, Dr. (Prof.) M. K. Gupta, Shailesh Kumar, Alok kumar, Ankit Yadav, Akshay Kumar (2024). Formulation And Evaluation Of Allicin Loaded Nanoparticles For Potential Antiseptic Properties. *Frontiers in Health Informatics*, 13 (7) 689-703

INTRODUCTION

The immune system can frequently prevent these viruses from proliferating within the body. If not, there could be significant harm. The type of pathogen determines how an illness spreads and what impact it has on the body. The immune system is a powerful barrier against pathogenic microorganisms. Although occasionally pathogens can outnumber the immune system's ability to fight them. At this time, an infection becomes dangerous. A few pathogens hardly make any difference. Others produce toxins or inflammatory substances that cause the body to react negatively. This diversity implies that although some infections are serious and life threatening, others can be mild and scarcely apparent. Some pathogens are treatment-resistant [1].

Viral infections

A virus infection leads to viral infections. Although there may be millions of distinct viral types, just 5,000 have been recognized by scientists thus far. In viruses, which are covered in a lipid (fat) and protein layer, a little amount of the genetic code is present. Viruses that invade a host join a cell after doing so.

As they enter the cell, they discharge their genetic material. This chemical makes the virus expand by making the cell force the virus to replicate. Dead cells release new viruses, which infect newly formed cells. [2].

Viruses might go dormant for a while before they start to replicate once more. The virus-infected person might seem to be entirely recovered, but if the virus reactivates, they could get ill once more [3].

Bacterial infections

Prokaryotes, which are single-celled microorganisms, include bacteria. There are at least 1 nonillion microorganism on Earth, according to experts. A nonillion consists of a 1 and 30 zeros. The biomass of the planet is largely made up of microorganisms. The three primary shapes of bacteria are:

- Cocci are these round organisms.
- Bacilli are these rod-shaped organisms.
- Spiral: Spirilla are coiled bacteria. Scientists refer to a spirillum as a spirochete if its coil is unusually compact.

Many of the trillions of bacterial types that exist do not harm people. Some of them exist safely within the human body, such as in the stomach or airways. Some "good" bacteria fight off "bad" bacteria to stop them from spreading disease [4].

Fungal infection

A fungus is typically a multicellular pathogen that consumes and absorbs organic materials using an enzyme. Other species, such as fungi, only have one cell. In most cases, spores with a single cell serve as the main form

of fungal reproduction. There are about 5.1 million kinds of fungus, according to a reliable source. Many fungus infections start in the epidermis and some spread to the deeper layers of the skin. Illnesses throughout the body or fungal illnesses, such as pneumonia, can occasionally result from inhaled yeast or mould spores. Also known as systemic infections, these are those. The beneficial bacteria that the body typically has serve to keep the balance of germs in check. These line the mouth, vagina, intestines, and other bodily cavities [9,15,17].

Pre-formulation studies

Physical appearance:

A qualitative test in which we describe the drug's color, and texture. These tests are important because if the appearance changes throughout manufacturing or storage, the quality of the drug may be compromised.

Melting point:

A tiny capillary tube filled with 0.1 gram of the drug, attached to the bottom of a thermometer positioned in the center of a heating bath,

The bath was steadily heated while being watched to see when melting started to occur.

Determination of the λ_{max} of allicin

For 72 hours, 0.1 grammes of pure medication were stirred at 25°C in a rotary shaker with 100 cc of methanol. Following equilibration, 0.45 m Millipore filters were used to filter the samples. Appropriately diluted with the appropriate solution, then analyzed using a UV- Visual Spectrophotometer to measure absorbance at various wavelengths (200 nm– 500 nm).

Standard calibration curve preparation:

100 mg/ml stock solution was prepared and then the working solution of different concentrations were prepared, and the absorbance was taken at 290 nm.

Determination of Aqueous Solubility

The estimation of allicin's solubility in water using the saturation shake- flask method.

A suitable concentration of allicin is diluted in distilled water with an acetate buffer pH 5.5, followed by centrifugation at 50 rpm for 48 hours at 37°C, filtration, and spectrophotometric analysis at 299 nm. Qualification was performed in triplicate.

Measuring lipophilicity

- To determine the lipophilicity of allicin, the protocol's recommended shake flask method was employed, with a few modifications.
- Basically, an optimum uniform amount of allicin was put to three different volumetric flasks, and then determined amounts of lipids such as stearic acid, prectrol, and dynasan 114 were simultaneously added to each flask.
- Centrifugation was performed on the obtained heterogeneous mixture for 48 hours at 50 rpm and 37 °C.
- A 0.22 m syringe filter was used to separate and filter the supernatant.
- The filter was then spectrophotometrically examined at 299 nm.
- Using a water and n-octanol partition system, the additional allicin partition coefficient was calculated.
- Measured volumes of n-octanol and aqueous buffer solution were added to a conical flask, which also contained a measured amount of allicin. The flask was shaken at regular intervals for 48 hours to achieve equilibrium, after which the liquid was added to a separating flask with one more shake and was left undisturbed to separate into two layers [13].
- The targeted measurement was then subjected to spectrophotometric analysis at 299 nm. The calculated

log10P ratio was used to determine the results for both phases.

- All qualifications taken in triplicate[8].

Fourier Transform Infrared (FTIR) Spectroscopy

- The spectrum of allicin and stearic acid are analyzed using the Win-IR, Bio-Rad FTS spectrophotometer, and both samples are combined with potassium bromide before being analyzed between 4000 and 400 cm¹.

Preparations of allicin loaded solid lipid nanoparticles (SLN)

- The solvent diffusion method stated protocol was used to generate the SLN, with a few alterations. In a nutshell, 5 ml of ethanol was mixed with a known amount of allicin and stearic acid, and then the mixture was heated on a water bath to 603 °C.
- The resulting solution was added with a syringe to 5 ml of aqueous poloxamer 188 solutions at 4 to 8°C while being magnetically agitated at 2000 rpm. Centrifugation at 2000 rpm for 30 min at 4°C was needed to recover SLN.
- It was then homogenized at high pressure using an APV 2000 homogenizer operating at 1200 bars after being obtained as a heterogeneous mixture.

Evaluation of SLN

Evaluation of entrapment efficiency

- The method was used to determine the EE of SLN loaded with allicin with just minor adjustments.
- Synthesized SLN was dried at room temperature before being dissolved in 10 ml of HPLC-grade ethanol using 5 mg of the dried material. The mixture was then filtered using 0.22 g capacity syringe filters. At 299 nm, allicin concentration was determined spectrophotometrically.
- Three copies of the qualification were completed, with the best one being selected for further consideration based on the degree of entrapment.

Physicochemical property

- The physicochemical characteristics of SLN dispersions were defined as the color, smell, pH, and solubility of SLN F6 in aqueous media.

Particle size and zeta potential

- With a few minor adjustments, the zeta potential and average particle size were computed using the recommended methods.
- At-room-temperature zeta potential/particle size analyzer analysis.
- The sample was prepared for analysis by dilution of SLN F6 with phosphate-buffered saline to maintain pH at 7.4.

Optical microscopy

Analysis of the modified formulation using optical microscopy A fluorescent lamp- equipped digital light optical microscope (Labomed LX-400) was used to investigate SLN F6 at a 100x magnification.

The major objective of the study was to determine if allicin SLN is effectively confined inside SLN dispersion with a homogeneous and uniform texture.

FTIR spectra of SLN F6

- A Win-IR, Bio-Rad FTS spectrophotometer was used to perform the SLN F6 spectrum analysis.
- Each sample is mixed with potassium bromide before being subjected to spectroscopic analysis between 4000 and 400 cm¹[6].

Preparation of gel

- The cited process was somewhat modified in order to produce the gel. In a nutshell, distilled water was used to dissolve Carbopol 934P, and stirring was done continuously for 30 minutes at a speed of 600 rpm. The next steps were adding methylparaben sodium(0.02% w/v) and propylparaben sodium (0.1% w/v).
- For 24 hours, a prepared gel base remained neglected. SLN F6 was then added to the carbopol gel bases and constantly shaken at 1000 rpm for 30 minutes with the necessary amounts of propylene glycol (5% w/w) and ethanol (1% w/w).
- Tri-ethanol amine (TEA) underwent one additional step in which the pH was maintained between 5.5 and 6.5 to stabilise the drug and it was completely mixed to create a translucent gel.
- The aim of developing the various gel forms was to achieve the best homogenous and uniform texture with steady physicochemical dependability in terms of leading moiety release %.
- The same procedure was utilised to make four formulations with different concentrations of carbopol.
- The table below lists the various SLN gel formulations available:

Table 1: Preparation of different formulations of solid lipid nanoparticles containing gel

Carbopol 934 %(w/v)	Formulation Code
0.5	Gr.1
1	Gr.2
1.5	Gr.3
2	Gr.4

Characterization of gel

1. Determination of pH

- With the aid of a digital pH metre, the gel's pH was assessed according to procedure.
- The glass electrode of the pH metre was submerged in an improved SLN gel formulation and rotated to ascertain the gel's pH.

2. Determination of viscosity

- The following modifications were made to the usual methodology for evaluating gel viscosity.
- In short, the obtained SLN gel was assessed physically, and its viscosity was assessed using a Brookfield viscometer.

3. Calculating the trapping effectiveness

- The % EE of several gel preparation batches was calculated by measuring the amount of free mass drug in the diffused phase of the gel solution following centrifugation.
- To guarantee effective drug extraction in ethanol, 1g of gel diffused with ethanol and vortexes for 5 minutes.
- After that, the prepared mixture underwent centrifugation at a speed of 15000 rpm for 60 minutes at a temperature of 4 °C.
- Supernatant was removed from the centrifuged mixture and allowed to undergo spectrophotometric examination at 299 nm for quantitative measurement.

4. Spreadability

- With certain modifications to the methodology given, the Spreadability of the gel was determined.
- In a nutshell, a second plate is concentrically positioned above the first, with 500 mg of the optimized formulation placed on the acrylic plate in the center.

- A weight of about 500 g was applied to the plate above for a short while.
- According to increases in diameter brought on by the spreading of gels and the note attained diameter of the disseminated gel, Spreadability of gel is calculated[12].

5. *In-vitro* drug release and kinetics study

- Using the dialysis bag technique, in-vitro drug release profiling methods were used to assess the drug release and kinetics profiling of the optimized formulation (SLN G3) gel.
- 1g of correctly weighed gel sample was deposited on a cellulose dialysis membrane.
- A membrane that has been thread-tied and put into a flask with 50 ml of ethanol and phosphoric buffer solution.
- Container placed to magnetic stirrer at 37 °C with constant stirring at 50 rpm. Higuchi and Korsemeyer-Peppas, zero-order, and first-order kinetic models, as well as other models were used to statistically analyse the in-vitro drug release profiles of the developed allicin -loaded SLN gel formulation.
- To shed insight on the process underlying drug release profiles, kinetics models were statistically calculated. High regression coefficient values were shown to be particularly useful for initiating and approving kinetics orders.

6. Scanning Electron Microscopy

- The morphological analysis is performed on SLN G3 and analysed by SEM using amodified version of the usual technique.
- A little SLN gel sample was applied to a glass stub and vacuum-dried.
- Following that, a stub containing a sample was placed in a SEM chamber that was coated in gold-palladium. The sample was then examined under a microscope at a 10 kV accelerating voltage.

7. Statistic study:

One-way ANOVA was used for the statistical analysis of the data. When $p < 0.05$, a difference was deemed statistically significant[5,10,16].

RESULTS AND DISCUSSIONS

Pre-formulation study of drug

Organoleptic properties studies:

Table 2: Organoleptic studies of the Allicin

S. No.	Parameters	Results
1.	Appearance	Solid
2.	Texture	Powder
3.	Melting point	155.2 °C
4.	Color	White

λ_{max} determination:

While performing the experiment, the maximum absorbance was found at 299nm. Hence the further studies were carried out at this wavelength.

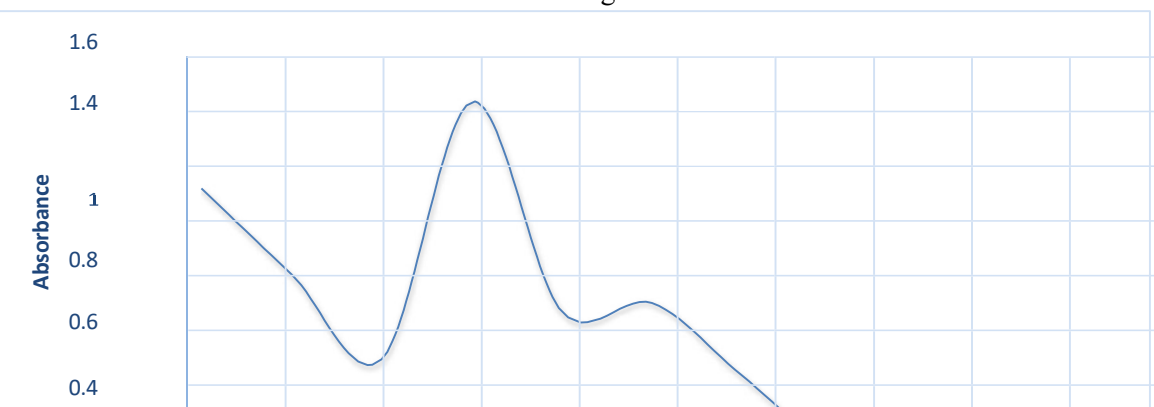


Figure 1: UV-Vis analysis for λ_{max} determination
Table 3: Standard calibration curve preparation of Allicin

Absorbance	Conc. (mg/ml)
0.072	10
0.147	20
0.213	30
0.285	40
0.361	50
0.432	60

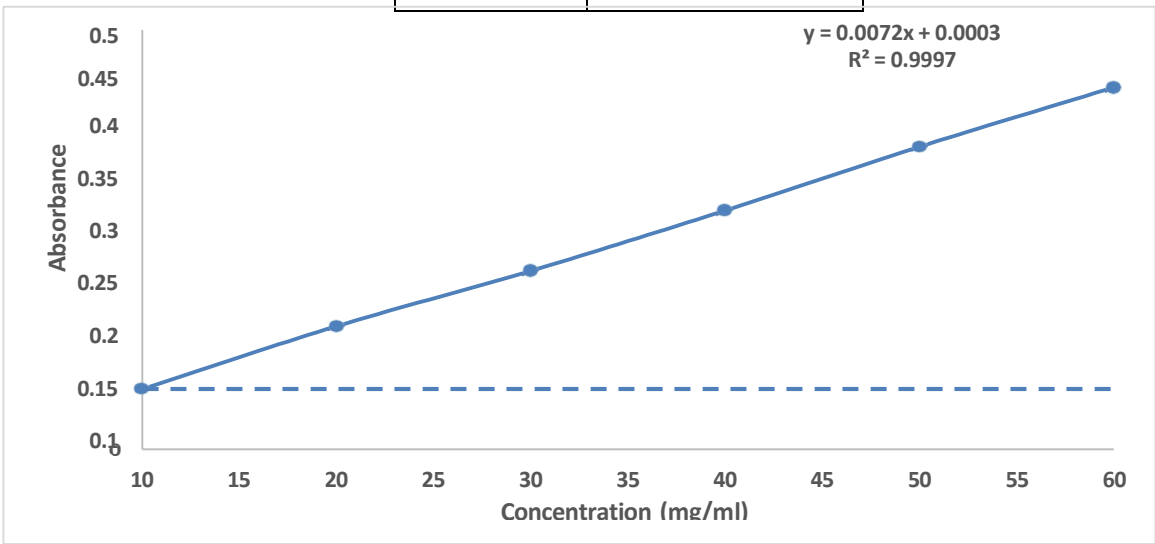


Figure 2: Absorption maxima of allicin and regression coefficient against the different concentration of allicin ($\mu\text{g/ml}$)
FTIR Spectrum analysis:

Table 4: FTIR interpretation of allicin

Characteristics Peaks	Observed(cm^{-1})	Reported (cm^{-1})
Para-C-H distribution	820.41	800-860
C-Cl Stretch	759.46	800-600 -
C=C-C Aromatic Ring Stretch	1471.35	1450-1510
C=C aromatic Stretch	1554.35	1650-1450
C \equiv N Stretch	2198.82	2400-2100
C-H Stretch	2979.43	3000-2850

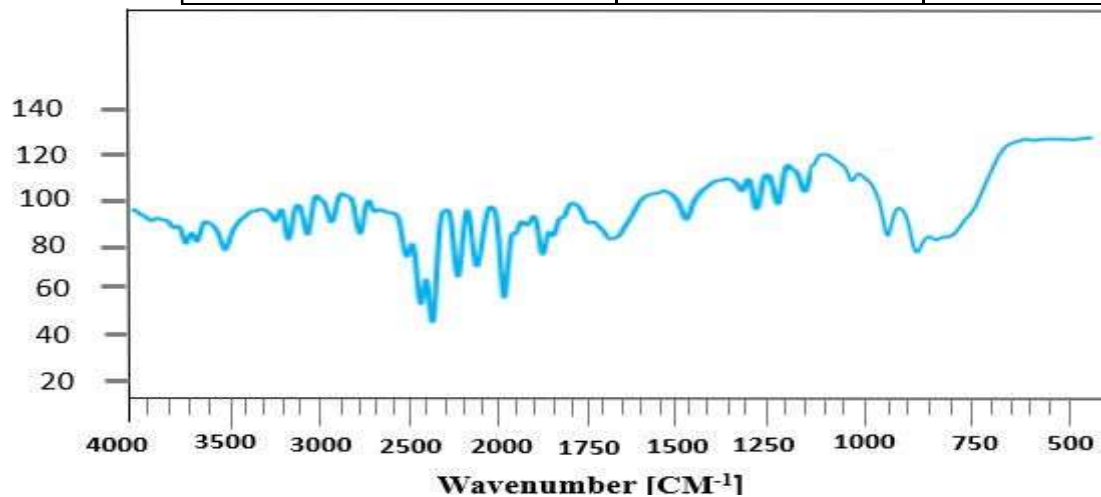


Figure 3: FTIR spectrum of allicin

The FTIR spectra are interpretation of stearic acid shown in Figure and Table, principal IR absorption peaks of stearic acid at 2915.20cm^{-1} (C–H stretch alkanes), 2848.02 cm^{-1} (C-H stretch aldehyde), 1700.89 cm^{-1} (C=O stretch saturated), 1471.59cm^{-1} (C-C stretch), 1295.47 cm^{-1} (C-O stretch, aromatic aster), 936.42 cm^{-1} (O-H bend), 719.89cm^{-1} (C=C bend) and 547.03 cm^{-1} (C-I stretch) were all detected in spectra of stearic acid. These detected principal peaks confirmed purity and authenticity of stearic acid as like reported data.

Development of the method for allicin loaded solid lipid nanoparticles(SLN)

Table 5: Making various allicin solid lipid nanoparticles

SLN code	Different leading reagent concentrations for the production of SLN		
	Stearic acid % (w/v)	Poloxomer 188 %(w/v)	Allicin % (w/v)
F1	0.5	1	1
F2	0.7	1	1
F3	1	1	1
F4	2	1	1
F5	1	0.5	1
F6	1	0.7	1
F7	1	1.5	1
F8	1	2	1

Evaluation of SLN

Evaluation of entrapment efficiency of SLN

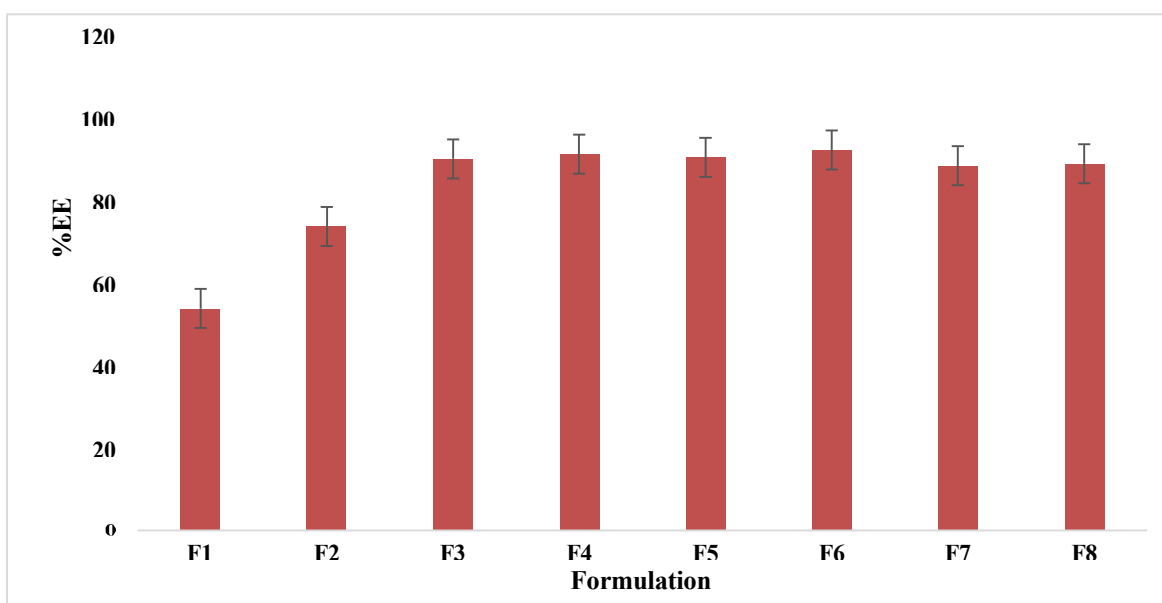


Figure 4: Allicin 's percentage entrapment effectiveness in SLN

Physicochemical property

The physicochemical properties of the SLN F6, including colour, scent, pH stability, and water solubility, were assessed. It also has a good pH stability, a homogeneous texture, a transparent white tint, and a pleasant fragrance.

Size distribution identification

The nano ZS90 zetasizer instrument was used to test the zeta potential and analyse the particle size of allicin SLN. One of the zeta potentials can be used to predict the physical stability of nanoparticles. High zeta potential values are necessary for the stability of nanoparticle systems, which suggests that they will improve the stability of nanosystems by serving as a repulsive force between the particles.

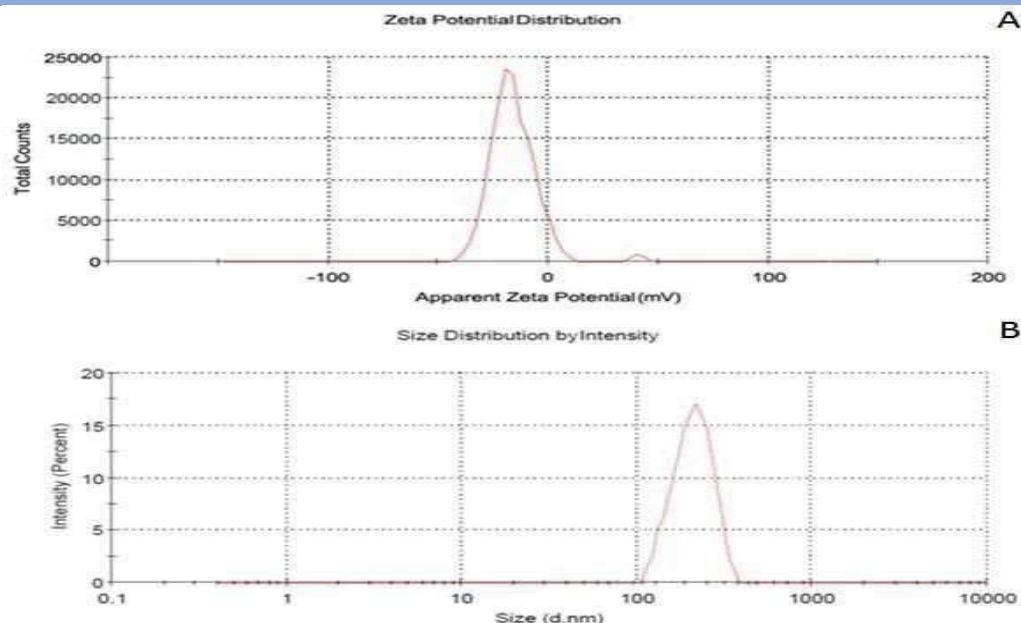


Figure 5: allicin SLN F6's zeta potential, particle size, and size distribution

Optical microscopy

With the use of a digital light optical microscope and optical microscopy of the optimised formulation, SLN F6, observation using 100x magnification reveals that allicin SLN is effectively localised with homogenous and uniform texture inside SLN dispersion.

Drug-excipient comparability study by FTIR

To ascertain any potential interactions between the medicine and drug additives, FTIR analysis of SLN F6 was conducted. The reported referenced values are strongly supported by spectral data. 52

Table 6: FTIR interpretation of SLN F6

Observed(cm ⁻¹)	Characteristics Peaks	Reported (cm ⁻¹)
2955.75 2914.97 2848.05	C-H stretch	2850 – 3000
2201.52	C≡N Stretch	2100 – 2400
1698.03	C=C alkene stretch	1650 – 2000
1463.82	C=C Aromatic stretch	1450 – 1650
609.29	C-Cl stretch	550 – 850

SLN gel
assessment

optimisation and

Unpretentious and reliable preparation methods for several SLN gels were discovered. First, the effectiveness of the four different



SLN gel preparations, designated as G1, G2, G3, and G4, was assessed in order to measure the percentage of allicin entrapment spectrophotometrically at 299 nm.

Figure 6: Visual appearance of SLN G3 gel

In vitro drug release and kinetics study

To predict release mechanism and contrast release profile, statistical models are frequently used. Drug in-vitro release profile was tested for 24 hours in a buffer system that had been established. According to Figure and Table, allicin desolvation percentages from SLN rise proportionately over time. Evidence from release profiles demonstrates that the created SLN is capable of releasing drugs in a controlled manner.

In vitro drug release and kinetics study

To predict release mechanism and contrast release profile, statistical models are frequently used. Drug in-vitro release profile was tested for 24 hours in a buffer system that had been established. According to Figure and Table, allicin desolvation percentages from SLN rise proportionately over time. Evidence from release profiles demonstrates that the created SLN is capable of releasing drugs in a controlled manner.

Table 7: Drug release percentage profiles for G3 and control gel.

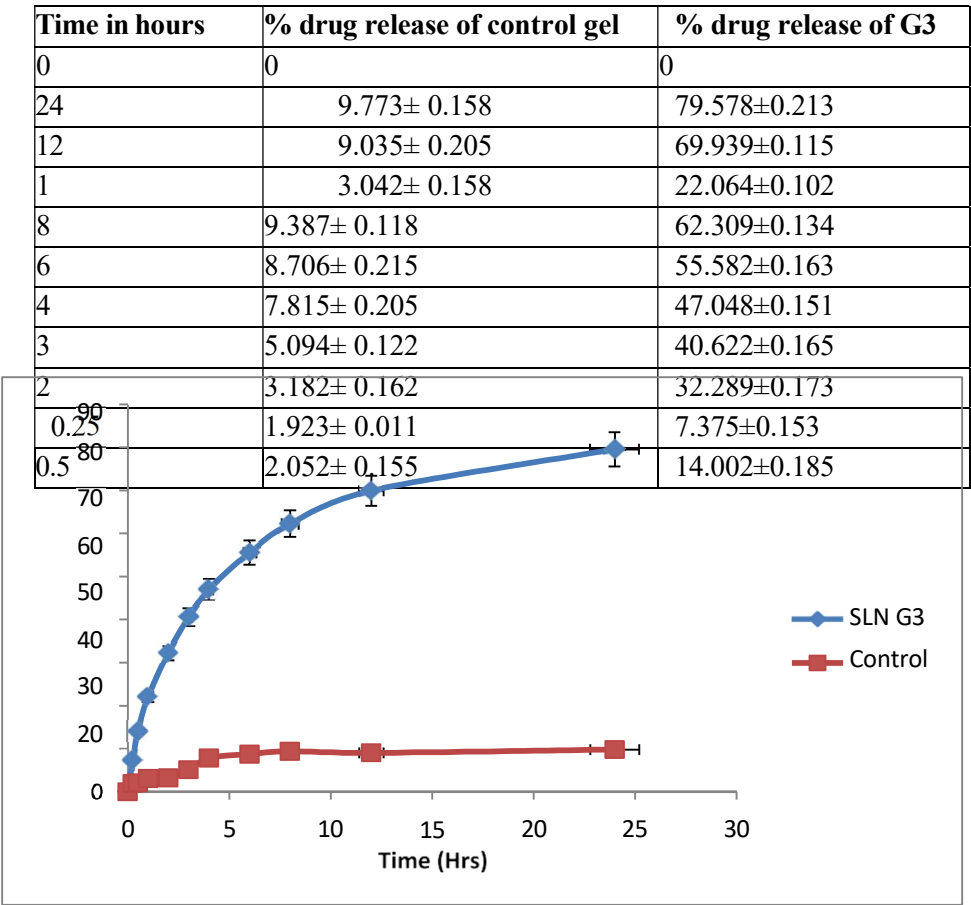


Figure 7: In-vitro drug release profile of SLN gel and control gel

Additionally, a drug release profile for optimised formulation using zero- order, first- order, Higuchi, and Kros-mayer-Peppas kinetic models was used. The collected data were statistically analysed with regard to rate constant and greatest correlation in order to state kinetics profile of drug release. According to earlier hints of evidence, this conclusion is nearly identical to virtuous covenant. Figure depicts the

kinetics order for the SLN G3 gel graphically.

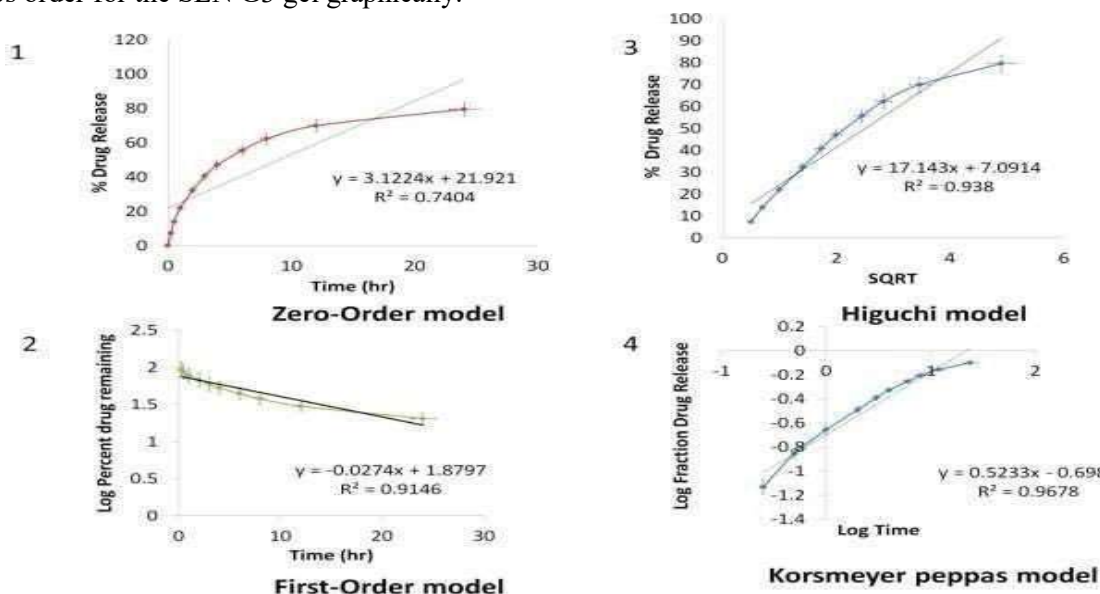


Figure 8: kinetics order of SLN G3 gel

FTIR examination of the SLN G3 gel

The FTIR spectral examination of SLN gel G3 was successful in identifying potential drug-drug additive interactions since the spectral data it produced matched those of allicin and stearic acid.

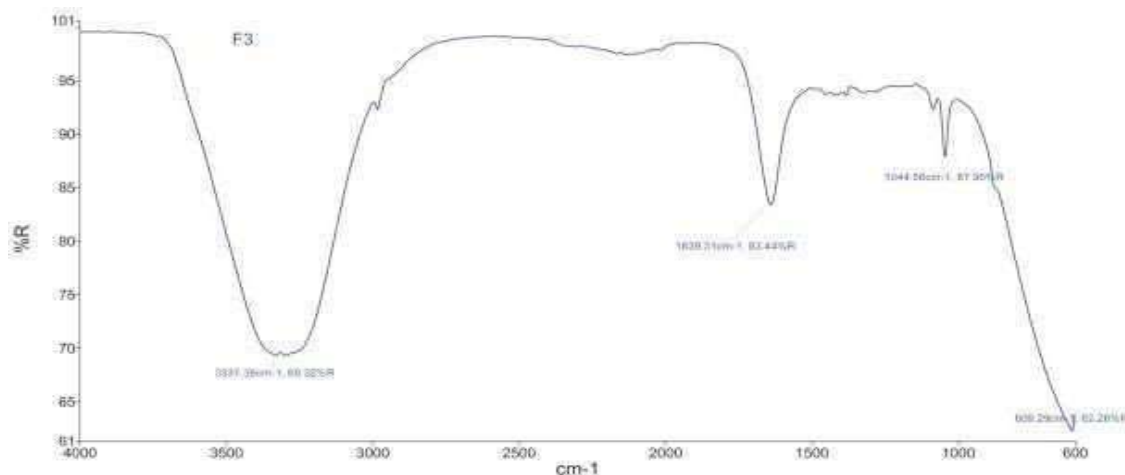


Figure 9: FTIR spectra of SLN gel G3

Table 8: FTIR interpretation of SLN G3 gel

Characteristics Peaks	Reported (cm ⁻¹)	Observed (cm ⁻¹)
N-H stretch	3300 – 2400	3331.36
C=C stretch	1638 – 1648	1639.31
CO - O - CO stretch	1040 – 1050	1044.56
C - Cl stretch	550 – 850	609.26

Scanning electron microscopy

Figure illustrates the morphology of the improved formulation as confirmed by SEM analysis. Allicin -loaded SLN in gel had a spherical shape and a smooth surface, according to SEM tests.

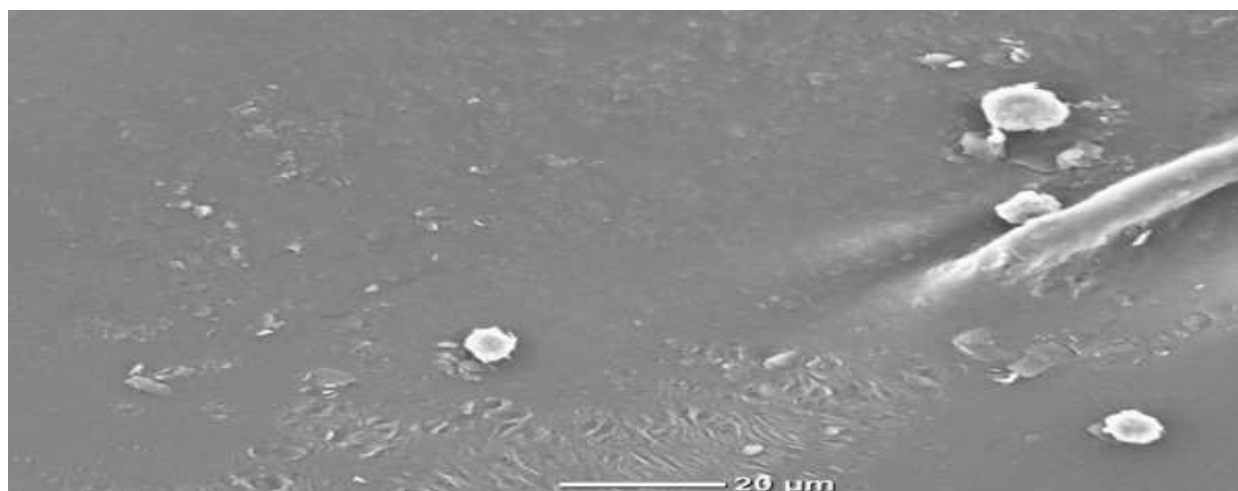


Figure 10: SEM analysis of SLN G3 gel

DISCUSSION

- While performing the preformulation studies it was found that, the Allicin insolid in appearance and in powdered form. The melting point of Allicin is 155.2 °C and it is white in colour.
- Further the maximum absorbance was found at 299 nm. Hence the further studies were carried out at this wavelength. The calibration curve of Allicin was prepared and following equation was obtained; $y=0.0072x+0.0003$ and R^2 is 0.9997.
- To assess the physicochemical characteristics of the medicine, allicin, physicochemical studies were carried out. studies to assess the compatibility of allicin with hydrophilic and lipophilic environments. The results demonstrate that allicin has a low solubility potential in water, where it was found to be 0.00585 0.293 mg/ml, and that it is soluble in stearic acid, prectrol, and dynasan 114, where it was found to be 23.754 0.47, 18.314 0.85, and 22.875 0.32 mg/ml, respectively. Furthermore, allicin's non- aqueous solubility in n-octanol was 17.984 0.52 mg/ml. The log10P values for allicin were simultaneously 3.98, 3.30, 3.87, and 3.65 in stearic acid, prectrol, dynasan 114, and n-octanol.
- The technique uses a variety of modified nano-precipitation techniques, including cooling sonication probe and nano-precipitation, to optimise SLN with regard to EE of allicin at both treatment segments. 4°C and 25°C are used to adjust the temperature in both portions. Instantaneous hyphenation with anti-solvent

causes quick precipitation when organic phase is added to aqueous phase that has been kept at 4°C.

The initial nano-precipitation phase had a regulated temperature, which aided in achieving homogeneity. By reducing the size of bigger crystals and bead milling aggregation, high-pressure homogenization helps to achieve uniform homogeneity. Additionally, the procedure was preserved step by step using stearic acid and poloxamer 188 (w/v) concentration variations ranging from 0.5-2%.

- Allixin was initially characterised spectroscopically and physicochemically in pre- formulation experiments. Percentage EE of allixin was calculated following the successful production of various batches of nanoparticles. EE assessed spectrophotometrically at 299 nm as a percentage.
- The subsequent findings show that SLN F6 and SLN F1 had the highest and lowest percentages of EE of allixin loaded SLN, respectively, by 92.13% and 53.78% w/w. A study quoted by Ige et al. revealed the maximum EE was between 90 and 95% w/w. As a result, SLN F6 was chosen as an optimised SLN based on the percentage of drug entrapment and was then put through additional testing, which looked at its physicochemical characteristics and gel formation. Figure displays visually the percent of all SLN groups that were drug-entrapped.
- To ascertain any potential interactions between the medicine and drug additives, FTIR analysis of SLN F6 was conducted. The main absorption peaks of allixin are found in the following spectrum ranges: 2955.75 cm⁻¹ for C-H stretching, 2523 and 2647 cm⁻¹ for S-H stretching, 2201.52 cm⁻¹ for CN stretching, 1556.90 cm⁻¹ for C=N stretching, 1471.88 cm⁻¹ for C=C aromatic ring stretching, and 720.33 and 1101.29 cm⁻¹ for C-Cl stretching. While the main stearic acid absorption peaks were discovered at 2914.97 cm⁻¹ and 2848.05 cm⁻¹ in the high-frequency range, attributed to the asymmetric and symmetric stretching vibrations of the -CH₂- band, respectively, and at 1698.03 cm⁻¹ for the -COOH stretching in the low-frequency zone. After successful SLN synthesis, there are no more alterations to allixin, according to spectral analysis of optimised SLN. The reported referenced values are strongly supported by spectral data.
- Unpretentious and reliable preparation methods for several SLN gels were discovered. First, the effectiveness of the four different SLN gel preparations, designated as G1, G2, G3, and G4, was assessed in order to measure the percentage of allixin entrapment spectrophotometrically at 299 nm. The data obtained reveals that SLN G3 with 1.5% carbopol w/w has the highest drug entrapment percentage (91.39%). After that, the improved formulation is further assessed for physiochemical characteristics like spreadability, viscosity, pH, and appearance. The data obtained shows that the G3 gel's viscosity was determined to be 369cP, which is comparable to the gel viscosity reported by Jana et al. Further spreadability testing revealed that the created SLN gel had a good spreadability factor of 4.5, making it an effective topical formulation. From the perspective of patient compliance, spreadability is one of the critical physical qualities of any topical preparation.

To predict release mechanism and contrast release profile, statistical models are frequently used. Drug in-vitro release profile was tested for 24 hours in a buffer system that had been established.

According to Figure and Table, allixin desolvation percentages from SLN rise proportionately over time. Evidence from release profiles demonstrates that the created SLN is capable of releasing drugs in a controlled manner.

- The homogenous drug entrapment across systems is the basis for the slow release of the leading moiety from the majority of SLN forms. The same idea is put out by Ekambaram et al., who assert that a regulated drug desolvation profile can be achieved when the drug is evenly distributed throughout the lipid matrix. Because Poloxamer 407 has a higher HLB value than Cremophor RH 40, it is significantly more effective against the rate of drug release from SLN. Poloxamer 407 also has a high external spreadability, which reduces the impact of interfacial tension between SLN and the dissolution medium.

Additionally, it speeds up drug breakdown and decreases drug particle buildup. Additionally, the lipid mass in SLN can boost drug desolvation strength and modulate nanoparticle size. The length of drug disassociation is lengthened by the thickness of the lipid around the nanoparticle, prolonging the effects of drug release.

- Additionally, a drug release profile for optimised formulation using zero-order, first-order, Higuchi, and Krosmayer-Peppas kinetic models was used. The collected data were statistically analysed with regard to rate constant and greatest correlation in order to state kinetics profile of drug release.
- All models, with the exception of the zero-order equation, had the best-fitting line. The statistics that follow describe the controlled or regular distribution of drugs from homogeneous matrix systems and explain why they spread more slowly. Observations led researchers to the conclusion that SLN G3 is a considerably more effective option for a topical medication delivery formulation.

According to earlier hints of evidence, this conclusion is nearly identical to the virtuous covenant. Figure depicts the kinetics order for the SLN G3 gel graphically.

- The FTIR spectral examination of SLN gel G3 was successful in identifying potential drug-drug additive interactions since the spectral data it produced matched those of allicin and stearic acid. While the primary absorption peaks of stearic acid have been assigned at 2932.49 cm⁻¹ and 2863.16 cm⁻¹ in the high-frequency area, which are attributed to asymmetric and symmetric stretching vibrations of the -CH₂- band, and 1639.31 cm⁻¹ for -COOH stretching in the low-frequency zone. Even after the consecutive creation of topical gel, spectral analysis of the optimised formulation G3 demonstrates that no more drug-drug additive interactions are feasible. Therefore, it may be argued that spectra demonstrate the SLN G3 gel's validity and purity.

Figure of SEM illustrates the morphology of the improved formulation as confirmed by SEM analysis. The majority of vesicles are well-defined, discrete, spherical, and have extensive internal aqueous spaces. SEM examination reveals low density of nanoparticles, which may be caused by the dilution of nanosuspension prior to taking SEM images. Allicin-loaded SLN in gel had a spherical shape and a smooth surface, according to SEM tests.

REFERENCES

1. Khattab, A., & Ismail, S. (2016). Formulation and evaluation of oxiconazole mucoadhesive nanoemulsion based gel for treatment of fungal vaginal infection. *Int J Pharmacy and Pharm Sci*, 8, 33-40.
2. Chellapa, P., Mohamed, A. T., Keleb, E. I., Elmahgoubi, A., Eid, A. M., Issa, Y. S., & Elmarzugi, N. A. (2015). Nanoemulsion and nanoemulgel as a topical formulation. *IOSR J Pharm*, 5(10), 43-47.
3. Giongo, J. L., Vaucher, R. D., Ourique, A. F., Steffler, M. C., Frizzo, C. P., Henneinman, B. R. U. N. O., ... & Raffin, R. P. (2016). Development of nanoemulsion containing Pelargonium graveolens oil: Characterization and stability study. *Int J Pharm Pharm Sci*, 8, 271-6.
4. Lee, K. W., bin Omar, D., bt Abdan, Khalina, & Wong, M. Y. (2016). Physiochemical Characterization of Nanoemulsion Formulation of Phenazine and their Antifungal Efficacy against Ganoderma Boninense PER71 in vitro. *RESEARCH JOURNAL OF PHARMACEUTICAL BIOLOGICAL AND CHEMICAL SCIENCES*, 7(6), 3056-3066.
5. Chime, S. A., Kenechukwu, F. C., & Attama, A. A. (2014). *Nanoemulsions—advances in formulation, characterization and applications in drug delivery* (Vol. 3). chapter.
6. Mishra, R. K., Soni, G. C., & Mishra, R. P. (2014). A review article: on nanoemulsion. *World journal of pharmacy and pharmaceutical sciences*, 3(9), 258-274.
7. Da Costa, S., Basri, M., Shamsudin, N., & Basri, H. (2014). Stability of positively charged nanoemulsion formulation containing steroidal drug for effective transdermal application. *Journal of Chemistry*, 2014.
8. Sabale, V., & Vora, S. (2012). Formulation and evaluation of microemulsion-based hydrogel for topical delivery. *International journal of pharmaceutical investigation*, 2(3), 140.

9. Derle, D. V., Burade, K. B., Kotwal, R. S., & Gaikwad, V. B. (2008). Formulation and evaluation of microemulsion based gel for topical delivery of Ketoconazole. *INDIAN DRUGS-BOMBAY*-, 45(2), 138.
10. Jufri, M., & Natalia, M. (2014). Physical stability and antibacterial activity of black cumin oil (*Nigella sativa* L.) nanoemulsion gel. *Int J Pharm Tech Res*, 1(6), 1162-9.
11. Patil, M. P., Shinde, G. P., Kshirsagar, S. J., & Parakh, D. R. (2015). Development and characterization of ketoconazole loaded organogel for topical drug delivery. *Inventi J*, 3, 1-10.
12. Fletcher, J., & Hill, A. (2007). Making the connection-particle size, size distribution and rheology. *Chemie. DE Information Service*, Retrieved October, 11.
13. Saberi, A. H., Fang, Y., & McClements, D. J. (2013). Fabrication of vitamin E-enriched nanoemulsions: factors affecting particle size using spontaneous emulsification. *Journal of colloid and interface science*, 391, 95-102.
14. Kadian, R. E. N. U. (2018). Nanoparticles: a promising drug delivery approach. *Asian J Pharm Clin Res*, 11(1), 30-35.
15. Lee, K. W., bin Omar, D., bt Abdan, Khalina, & Wong, M. Y. (2016). Physiochemical Characterization of Nanoemulsion Formulation of Phenazine and their Antifungal Efficacy against *Ganoderma Boninense* PER71 in vitro. *RESEARCH JOURNAL OF PHARMACEUTICAL BIOLOGICAL AND CHEMICAL SCIENCES*, 7(6), 3056-3066.
16. Mhaske, R. A., & Sahasrabudhe, S. (2011). Identification of major degradation products of ketoconazole. *Scientia pharmaceutica*, 79(4), 817- 836.